Journal of Xenobiotics

MDPI

Article

Impact of Combined Polycyclic Aromatic Hydrocarbon and Metal Exposure on Semen Quality: The Role of PAH–Metal Interactions

Hueiwang Anna Jeng [1,*], Sinjini Sikdar [2] and Chih-Hong Pan [3]

[1] Joint School of Public Health, Old Dominion University, Norfolk, VA 23529, USA
[2] Department of Mathematics and Statistics, College of Sciences, Old Dominion University, Norfolk, VA 23529, USA; ssikdar@odu.edu
[3] School of Public Health, National Defense Medical Center, Taipei 11490, Taiwan; chihhongpan2012@gmail.com
* Correspondence: hjeng@odu.edu; Tel.: +1-757-683-4594

Abstract

The objective of this study was to examine the interactions between 16 polycyclic aromatic hydrocarbons (PAHs) and six metals, namely the xenobiotic metals cadmium (Cd), lead (Pb), and arsenic (As) and the essential metals copper (Cu), zinc (Zn), and selenium (Se), in relation to semen quality and sperm DNA fragmentation. PAH exposure was assessed using personal breathing-zone measurements, whereas metal exposure was quantified by measuring urinary metal concentrations. Semen quality, including sperm concentration, motility, vitality, and morphology, was evaluated, and sperm DNA fragmentation was quantified using the terminal deoxynucleotidyl transferase dUTP nick-end labeling assay. Multiple linear regression models, with false discovery rate (FDR) adjustment, were used to examine whether PAH–metal interactions were associated with semen quality and sperm DNA fragmentation. Several associations between PAH–metal interactions and semen quality reached nominal statistical significance ($p_{raw} < 0.05$); however, none remained statistically significant after FDR correction ($p_{FDR} \geq 0.05$). In contrast, the interaction between Se and benzo[a]anthracene (B[a]A) in relation to sperm DNA fragmentation was statistically significant at both the nominal and FDR-adjusted levels. Se modified the association between B[a]A exposure and sperm DNA fragmentation, attenuating the increase in sperm DNA fragmentation associated with B[a]A exposure.

Keywords: metals; polycyclic aromatic hydrocarbons; sperm DNA fragmentation

Check for updates

Academic Editor: Giovanni Forte

Received: 8 September 2026
Revised: 20 October 2026
Accepted: 20 October 2026
Published: 26 October 2026

Copyright: © 2026 by the authors. Licensee MDPI, Basel, Switzerland. This article is an open access article distributed under the terms and conditions of the Creative Commons Attribution (CC BY) license.

1. Introduction

Data collected over the past several decades indicate a troubling, progressive decline in male reproductive health, characterized by deteriorating semen quality parameters such as sperm count, motility, and normal morphology [1,2]. While lifestyle choices, genetics, and clinical pathologies account for a portion of these cases, epidemiological and toxicological evidence points toward environmental pollution as a critical, under-addressed driver of male fertility decline.

Heavy metals and polycyclic aromatic hydrocarbons (PAHs) are two of the most ubiquitous and hazardous classes of environmental pollutants. They frequently co-occur because both classes of chemicals are generated through similar combustion and high-temperature processes. Major emission sources include vehicular emissions, coal combustion, biomass burning, and waste incineration [3]. Their widespread co-occurrence creates

complex multi-pollutant mixtures in which interactions between heavy metals and PAHs may occur, potentially resulting in unique toxicological effects and increased health risks.

Both PAHs and heavy metals have been recognized as reproductive toxicants [4,5]. Epidemiological studies have reported that PAH exposure is associated with reduced semen quality and increased sperm DNA fragmentation. PAHs act as endocrine disruptors and can form DNA adducts in germ cells, leading to sperm DNA fragmentation and apoptosis. Heavy metals can induce testicular oxidative stress, disrupt the hypothalamic–pituitary–gonadal axis, and directly impair spermatogenesis [6]. When these distinct classes of pollutants coexist within a reproductive system, they may interact in complex ways through overlapping and intersecting mechanisms of toxicity and target male reproductive health at every stage—from pituitary hormone regulation to gamete genomic integrity [7,8]. They may act through shared biological pathways, such as oxidative stress, or simultaneously target different physiological processes [9,10]. Consequently, combined exposure to PAHs and heavy metals may produce additive or synergistic toxic effects, resulting in greater damage to the male reproductive system than would be expected from individual exposures alone [11]. For example, PAHs and heavy metals may concurrently target different cellular components or amplify common pathological pathways, such as excessive generation of reactive oxygen species (ROS), overwhelming the limited antioxidant capacity of seminal plasma and leading to oxidative damage [11,12].

Currently, there is a relative scarcity of scientific literature examining the interaction effects of PAHs and heavy metals on male reproductive health. This largely stems from logistical challenges of male reproductive epidemiology and difficulty in subject recruitment for well-characterization of exposure and semen sample collection. To fill the information gap, the objective of the study was to explore prospective interactions of co-exposure to PAHs and heavy metals on semen quality. The study examined interactions between individual PAHs and metals in relation to semen quality and DNA fragmentation, while adjusting for the remaining exposure variables.

2. Materials and Methods

2.1. Human Subjects

Coke oven workers are exposed to relatively high concentrations of coke-oven emissions and are a suitable population to examine the effects of co-exposure to PAHs and metals [12]. We selected the steel plant for subject recruitment because of its well-established operation for more than five decades; the existence of long-term occupational monitoring from the Taiwan Department of Labor; increased PAH levels detected in the coking areas, particularly near coke ovens and the blast furnace; and increased urinary metals detected in the coke oven workers [13]. Eligibility criteria included more than one year of employment in the plant, ages between 25 and 60 years old, no reproductive dysfunction, no infection during sampling, and no cancer. More than 90% of the subjects met the inclusion criteria and were eligible to provide biological samples from 2012 to 2013. However, based on the work schedule during the time of the personal breathing zone sampling, 38 subjects were randomly selected and included in the study. All participants were fully informed about the objective of the study and signed the consent form before screening and sampling took place.

2.2. Collection and Measurements of PAHs and Metals

Personal breathing zone air samples were collected to determine the PAH intake of the human subjects. Detailed air sampling procedures were described in prior studies [14]. Sixteen targeted PAH compounds, namely naphthalene (NAP), acenaphthylene (ACY), acenaphthene (ACE), fluorene (FLE), phenanthrene (PHE), anthracene (ANT), pyrene (PRY),

fluoranthene (FLA), benzo[a]anthracene (B[a]A), chrysene (CHR), benzo[b]fluoranthene (B[b]F), benzo[k]fluoranthene (B[k]F), benzo(a)pyrene (B[a]P), indeno[1,2,3-cd]pyrene (IND), dibenzo[a,h]anthracene (D[ah]A), and benzo[ghi]perylene (B[ghi]P), were quantified using a gas chromatogram quadruple mass spectrometer (GC/MS, Agilent Technologies 6890N, Agilent Technologies, Santa Clara, CA, USA) with an automatic sampler system [15]. Detailed analytical procedures were described in our prior studies [14].

Urine samples were collected to quantify the internal human exposure dose of the metal mixture, including As, Cd, Pb, Cu, Se, and Zn. We selected the metals based on the preliminary results from our environmental monitoring. Blank samples were collected and quantified for the metal mixture to ensure no contamination of the collection vessel. The urine samples were pretreated using an acid digestion procedure as follows: First, 500 μL of urine was transferred into a pre-cleaned 4 mL microtube and treated with an aliquot of concentrated nitric acid at room temperature for 20 min. Then, the mixture solution was diluted 1-, 1-, 1-, and 200-fold with deionized water for analysis of Cd, Pb, Cu, Se, and Zn, respectively. The metals in the mixture solution were quantified by inductively coupled plasma dynamic reaction cell mass spectrometry (ICP-MS) (Thermo Scientific, Waltham, MA, USA). The concentrations were adjusted with creatinine and reported as μg/g creatinine. Detailed analytical procedures with limits of detection were described in prior studies [13].

2.3. Semen Collection and Semen Quality Analysis

The participants were instructed to abstain from ejaculation for at least three days before sperm collection. Each semen sample was collected by ejaculation. Within one hour after the sampling of the ejaculate, a technician conducted all routine semen quality analyses in the hospital laboratory. Analysis was initiated after completion of liquefaction and within 30 min after ejaculation. All laboratory tests were done in a blind fashion. Sperm concentration was assessed using hemocytometers with an improved Neubauer ruling. Sperm counting was done using a Olympus phase-contrast microscope (Olympus Cooperation, Center Valley, PA, USA). At least 300 sperm were counted in each of the duplicate assessments. Sperm motility was classified using a four-category scheme: rapid progressive, slow progressive, non-progressive, and immotile. For the morphology assessment, three hundred sperm per sample were evaluated from air-dried Papanicolaou-stained preparations. Assessments were done under high magnification (×1000–1250) using a 100× high-resolution oil immersion objective and bright-field microscope optics. Sperm morphology was classified as either normal or abnormal. Abnormalities are recorded for the four defined regions of the spermatozoon (head, neck/midpiece, tail, and cytoplasmic residue) For sperm vitality analysis, at least 300 sperm per sample were assessed using eosin-stained preparations (Thermo Scientific, Waltham, MA, USA). Sperm that did not take up eosin were considered viable, whereas those stained with eosin were considered nonviable. Sperm vitality was calculated as the percentage of viable sperm among the total number of sperm assessed [16,17].

2.4. Detection of DNA Fragmentation

The terminal deoxynucleotidyl transferase-mediated dUTP nick-end labeling (TUNEL) assay was performed to detect both single- and double-stranded DNA breaks [18]. Briefly, a sperm pellet was obtained from 100 μL of semen by centrifugation at 250 × g for 5 min. The pellet was then resuspended in 1% HSA in phosphate-buffered saline (PBS). The sperm were permeabilized with 0.1% Triton X-100 in 0.1% sodium citrate at 4 °C for 2 min (Thermo Scientific, Waltham, MA, USA). The TUNEL reaction mixture (Roche Diagnostics, Mannheim, Germany) was then applied to the sperm cells. Each assay included both

positive and negative controls to ensure proper assay performance. For the positive control, sperm cells were treated with 50 µL of DNase solution. For the negative control, sperm cells were not treated with the TUNEL reaction mixture. Following incubation for 1 h at 37 °C, the sperm cells were examined using an Olympus BX61 fluorescence microscope (Olympus Corporation, USA). Sperm exhibiting fluorescence was considered positive for DNA fragmentation. At least 300 sperm cells were evaluated for each sample, and the percentage of sperm cells exhibiting DNA fragmentation was calculated.

2.5. Statistical Analysis

Quantitative analyses were conducted to summarize participant characteristics, sperm quality parameters, and the distributions of the measured PAHs and urinary metals. For outcome variables, natural log transformation was applied because they showed right-skewed distributions and deviations from normality. The log transformation was performed to improve adherence to linear regression assumptions, including approximate normality of residuals and stabilization of variance. PAH and metal concentrations were entered into the regression models as continuous variables on their original measurement scales without transformation. Multiple linear regression models were used to evaluate whether heavy metals (Cd, Pb, and As) or essential metals (Cu, Zn, and Se) modified the associations between individual PAHs and sperm quality outcomes. For each PAH–metal pair, an interaction term and the corresponding main effects were included in the model while adjusting for the remaining PAHs, the remaining metals, and potential confounders, including age, body mass index (BMI), smoking status, drinking status, education, and job site. Age and BMI were modeled as continuous variables. Education (less than high school vs. at least high school), smoking status (yes vs. no), drinking status (yes vs. no), and job site (topside vs. side oven) were included as binary variables. Because participants were concurrently exposed to multiple PAHs and metals, the remaining measured PAHs and metals were included as covariates in each interaction model to account for concurrent co-exposures and to estimate each PAH–metal interaction conditional on the other measured exposures. Potential multicollinearity was assessed using Spearman correlations and generalized variance inflation factors (GVIFs). Sensitivity to co-exposure adjustment was evaluated by refitting identified interaction models without the remaining PAHs and metals. The influence of individual observations on interaction estimates was assessed using Cook's distance. To facilitate interpretation of nominally significant interactions between PAHs and metals, dose–response relationships between each PAH and each sperm quality outcome were estimated by fixing the interacting metal at its 25th percentile (low exposure) and 75th percentile (high exposure), while holding all other covariates constant. Predicted values from the fitted regression models were used to generate interaction plots illustrating these dose–response relationships. All sperm quality outcomes were natural log-transformed prior to analysis to improve adherence to model assumptions. Given the exploratory nature of the interaction analyses and multiple hypothesis testing across multiple concurrent statistical comparisons, both nominal and false discovery rate (FDR)-adjusted results were evaluated [19,20]. For each sperm quality outcome and metal class, 48 PAH–metal interaction tests were performed, corresponding to 16 PAHs and three metals. The Benjamini–Hochberg procedure was applied separately within each outcome-metal-class analysis to the 48 interaction p-values to control the FDR. Both unadjusted p-values (p_{int}) and FDR-adjusted p-values (p_{FDR}) are reported for interactions identified as nominally significant. Associations attaining an unadjusted p-value of $p_{int} < 0.05$ but failing to meet the FDR threshold ($p_{FDR} \geq 0.05$) were classified as nominally significant and categorized as exploratory signals for future validation rather than confirmatory discoveries, whereas Benjamini–Hochberg FDR-adjusted $p_{FDR} < 0.05$ were considered statistically significant

after correction for multiple comparisons. All statistical analyses were performed using R version 4.5.0 (R Foundation for Statistical Computing, Vienna, Austria).

3. Results

3.1. Human Subject Characteristics

Table 1 shows the characteristics of the study participants. The average age was about 40 years; most participants were non-drinkers, and the majority had at least a high school education, while half were smokers. Table 2 summarizes the concentrations of PAH metabolites and metals, reporting the median, 25th percentile, and 75th percentile concentrations.

Table 1. Demographic characteristics and semen quality.

Characteristic	Subjects $N = 38$	25–75th
Age (in years), mean ± SD	48 ± 8	
BMI (kg/m^2), mean ± SD	25.2 ± 4.1	
Education (%)		
Less than high school	48.1	
At least high school	51.9	
Smoking status (%)		
No	46.2	
Yes	53.8	
Drinking status (%)		
No	59.6	
Yes	40.4	
Work duration (in years)	6.5	
Sperm quality, mean ± SD		
Volume (mL)	1.9 ± 1.0	1.1–2.6
Concentration (10^6/mL)	115.6 ± 98.9	46.6–142.1
Motility (% motile)	55.9 ± 19.2	47.3–68.8
Vitality (%)	73.1 ± 17.6	65.0–85.0
Normal morphology (% normal)	15.3 ± 3.0	2.5–6.5
DNA fragmentation (%)	38.9 ± 23.8	19.0–55.0

Table 2. PAH concentrations in the personal breathing zone and metal concentrations in urine.

Exposure Variables	Median	25–75th Percentile
PAHs (ng/m^3)		
Naphthalene (NAP)	11.03	2.53–32.12
Acenaphthylene (ACY)	200.43	144.87–304.55
Acenaphthene (ACE)	332.29	207.90–449.70
Fluorene (FLE)	3683.49	2642.10–5487.30
Phenanthrene (PHE)	5891.50	1992.10–8622.60
Anthracene (ANT)	336.95	297.20–379.60
Benzo[g,h,i]perylene (B[ghi]P)	3217.42	2453.00–3855.00
Benzo[k]fluoranthene (B[k]F)	487.10	377.30–593.10
Indenol[1,2,3-cd]anthracene (IND)	712.44	567.10–797.60
Pyrene (PYR)	813.39	737.00–911.50
Benzo[a]anthracene (B[a]A)	972.92	352.30–1871.10
Benzo[a]pyrene (B[a]P)	1855.44	1438.80–2285.70
Benzo[b]fluoranthene (B[b]F)	1242.35	770.80–1526.10
Chrysene (CHR)	912.51	818.70–980.30
Dibenz[a,h]anthracene (D[ah]A)	297.59	253.50–415.30
Fluoranthene (FLA)	4376.39	1106.80–9486.60

Table 2. *Cont.*

Exposure Variables	Median	25–75th Percentile
Metals (µg/g creatinine)		
Cd	0.90	0.60–1.35
Pb	6.58	2.94–12.69
As	135.82	69.50–234.67
Cu	16.14	9.73–25.88
Zn	693.80	226.97–982.40
Se	16.24	12.43–24.25

3.2. Interaction Between PAHs and Xenobiotic Metals

In terms of sperm concentration, several nominally significant interactions were identified. Nominally significant positive interactions were identified between Cd and PYR (β_{int} = 0.0117, p_{int} = 0.022), B[a]A (β_{int} = 0.0010, p_{int} = 0.004), and B[b]F (β_{int} = 0.0026, p_{int} = 0.003) (Table 3). These associations did not remain significant after FDR correction. The dose–response analysis showed that sperm concentration declined with increasing PYR concentration at both low (25th percentile) and high (75th percentile) Cd levels, with a steeper decline observed at the lower Cd level (Figure S1a). Similarly, sperm concentration decreased with increasing B[a]A concentration when Cd was fixed at its lower level (25th percentile), whereas an increasing trend was observed when Cd was fixed at its higher level (75th percentile) (Figure S1b). In contrast, sperm concentration increased with increasing B[b]F concentration at both Cd levels, with a more pronounced increase observed at the higher Cd level (Figure S1c). Nominally significant positive interactions were also observed between Pb and NAP (β_{int} = 0.0024, p_{int} = 0.045), IND (β_{int} = 0.0003 p_{int} = 0.013), and B[a]A (β_{int} = 0.00007, p_{int} = 0.040), whereas a nominally significant negative interaction was identified between Pb and D[ah]A (β_{int} = −0.0007, p_{int} = 0.033) (Table 3). None of these interactions remained statistically significant after FDR correction. The dose–response analysis showed that sperm concentration increased with increasing NAP concentration when Pb was fixed at its higher level (75th percentile), whereas it decreased when Pb was fixed at its lower level (25th percentile) (Figure S2a). Similar dose–response patterns were observed for the interactions between Pb and IND and between Pb and B[a]A, with sperm concentration increasing at the higher Pb level but decreasing at the lower Pb level (Figure S2b,c). In contrast, the dose–response relationship for the Pb-D[ah]A interaction showed that sperm concentration declined with increasing D[ah]A concentration at both Pb levels, with a more pronounced decline observed when Pb was fixed at its higher level (75th percentile) (Figure S2d).

In terms of sperm motility, several nominally significant PAH–metal interactions were identified. Nominally significant negative interactions were observed between B[ghi]P and Cd (β_{int} = −0.0004, p_{int} = 0.008) and between B[ghi]P and As (β_{int} = -2.35×10^{-6}, p_{int} = 0.019) (Table 3). These interactions did not remain statistically significant after FDR correction and were therefore interpreted as exploratory findings. The dose–response analysis showed that sperm motility declined with increasing B[ghi]P concentration when Cd was fixed at its higher level (75th percentile), whereas a slight increase in motility was observed when Cd was fixed at its lower level (25th percentile) (Figure S3a). Similarly, sperm motility decreased with increasing B[ghi]P concentration at both the low (25th percentile) and high (75th percentile) As levels, although the decline was more pronounced at the higher As level (Figure S3b).

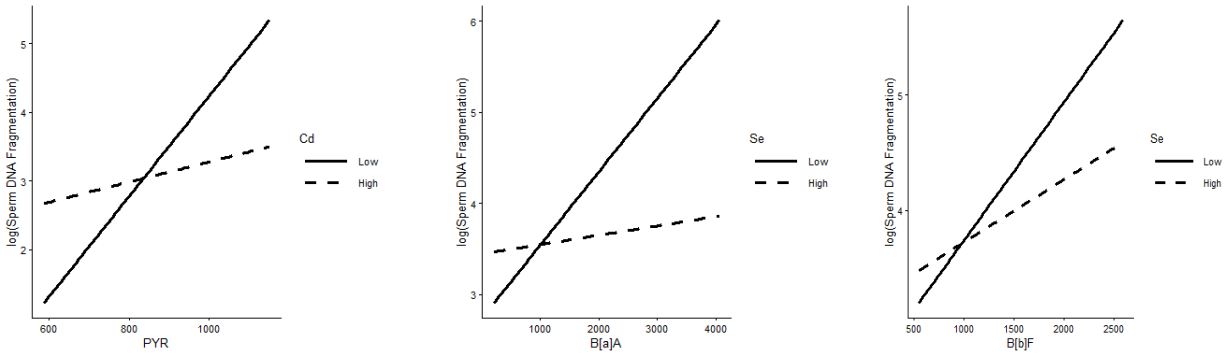
Table 3. Interaction between PAHs and metals in relation to sperm quality and sperm fragmentation.

Sperm Quality	Interaction	β_{int}	95% C.I.	p_{int}	p_{FDR}
Concentration	NAP Pb	0.0024	(0.00007, 0.0048)	0.045	0.274
	B[a]A × Pb	0.00007	$(3.92 \times 10^{-6}, 0.0001)$	0.040	0.274
	IND × Pb	0.0003	(0.00009, 0.0006)	0.013	0.208
	D[ah]A × Pb	−0.0007	(−0.0013, −0.00007)	0.033	0.274
	B[a]A × Cd	0.0010	(0.0004, 0.0015)	0.004	0.096
	B[b]F × Cd	0.0026	(0.0012, 0.0040)	0.003	0.096
	PYR × Cd	0.0117	(0.0022, 0.0211)	0.022	0.264
	NAP × Cu	0.0014	(0.0002, 0.0025)	0.027	0.672
	ACY × Se	−0.0005	(−0.0009, −0.00004)	0.037	0.672
Motility	B[ghi]P × Cd	−0.0004	(−0.0007, −0.0002)	0.008	0.384
	B[ghi]P × As	-2.35×10^{-6}	$(-4.19 \times 10^{-6}, -5.01 \times 10^{-7})$	0.019	0.456
	B[ghi]P × Cu	−0.00003	$(-0.00005, -8.54 \times 10^{-7})$	0.044	0.930
Normal morphology	ACY × Cd	−0.0073	(−0.0133, −0.0012)	0.026	0.923
	ACY × Cu	−0.0005	(−0.0011, −0.00003)	0.042	0.451
	PYR × Cu	−0.0004	(−0.0008, −0.00006)	0.027	0.451
	FLA × Cu	-7.62×10^{-6}	$(-0.00001, -9.37 \times 10^{-7})$	0.031	0.451
	PHE × Cu	-9.45×10^{-6}	$(-0.00002, -1.63 \times 10^{-6})$	0.024	0.451
	B[k]F × Se	0.0004	$(8.04 \times 10^{-6}, 0.0009)$	0.047	0.451
Vitality	B[ghi]P × As	-1.47×10^{-6}	$(-2.71 \times 10^{-6}, -2.28 \times 10^{-7})$	0.027	0.798
	B[ghi]P × Cu	−0.00002	$(-0.00003, -4.27 \times 10^{-6})$	0.018	0.864
Sperm DNA fragmentation	PYR × Cd	−0.0078	(−0.0148, −0.0007)	0.035	0.941
	B[b]F × Se	−0.00006	$(-0.0001, -6.30 \times 10^{-6})$	0.033	0.786
	B[a]A × Se	−0.00006	(−0.00009, −0.00004)	0.001	0.048

In terms of sperm morphology, a nominally significant negative interaction was observed between ACY and Cd ($\beta_{int} = -0.0073$, $p_{int} = 0.026$) (Table 3). After FDR correction, this interaction effect did not remain significant. The dose–response analysis showed that normal sperm morphology declined with increasing ACY concentration when Cd was fixed at its higher level (75th percentile), whereas an increasing trend was observed when Cd was fixed at its lower level (25th percentile) (Figure S4a).

In terms of sperm vitality, a nominally significant negative interaction was observed between B[ghi]P and As ($\beta_{int} = -1.47 \times 10^{-6}$, $p_{int} = 0.027$) (Table 3). This interaction did not remain significant after FDR correction. The dose–response analysis showed that sperm vitality declined with increasing B[ghi]P concentration at both low (25th percentile) and high (75th percentile) As levels, with a more pronounced decline observed at the higher As level (Figure S5a).

In terms of DNA fragmentation, a nominally significant negative interaction was observed between PYR and Cd ($\beta_{int} = -0.0078$, $p_{int} = 0.035$) (Table 3). This interaction did not remain significant after the FDR correction. The dose–response analysis showed that sperm DNA fragmentation increased with increasing PYR concentration at both low (25th percentile) and high (75th percentile) Cd levels, with a more pronounced increase observed at the lower Cd level (Figure 1a).



(**a**) (**b**) (**c**)

Figure 1. Dose–response trends between PAH exposures and sperm DNA fragmentation by both xenobiotic and essential metal exposure concentrations. (**a**) The dose-response trends between PRY exposure and sperm DNA fragmentation at different levels of Cd exposure; (**b**) The dose-response trends between B[a]A exposure and sperm DNA fragmentation at different levels of Se exposure; (**c**) The dose-response trends between B[b]F exposure and sperm DNA fragmentation at different levels of Se exposure.

3.3. Interaction Between PAHs and Essential Metals

In terms of sperm concentration, a nominally significant positive interaction was observed between Cu and NAP (β_{int} = 0.0014, p_{int} = 0.027), whereas a nominally significant negative interaction was identified between Se and ACY (β_{int} = −0.0005, p_{int} = 0.037) (Table 3). However, these findings did not remain significant after FDR correction. The dose–response analysis showed that sperm concentration increased with increasing NAP concentration at both low (25th percentile) and high (75th percentile) Cu levels, with a steeper increase observed at the higher Cu level (Figure S6a). In contrast, sperm concentration increased with increasing ACY concentration when Se was fixed at its lower level (25th percentile), whereas a slight decline was observed when Se was fixed at its higher level (75th percentile) (Figure S6b).

In terms of motility, a nominally significant negative interaction was identified between B[ghi]P and Cu (β_{int} = −0.00003, p_{int} = 0.044) (Table 3). This interaction did not remain significant after FDR correction. The corresponding dose–response analysis showed that sperm motility decreased with increasing B[ghi]P concentration when Cu was fixed at its higher level (75th percentile), whereas a slight increasing trend in sperm motility was observed when Cu was fixed at its lower level (25th percentile) (Figure S3c). No other nominally significant interactions were observed between the PAHs and either xenobiotic or essential metals on sperm motility.

In terms of normal sperm morphology, several nominally significant interactions were identified, including negative interactions between Cu and ACY (β_{int} = −0.0005, p_{int} = 0.042), PYR (β_{int} = −0.0004, p_{int} = 0.027), FLA ($\beta_{int} = -7.62 \times 10^{-6}$, p_{int} = 0.031), and PHE ($\beta_{int} = -9.45 \times 10^{-6}$, p_{int} = 0.024), and a positive interaction was observed between Se and B[k]F (β_{int} = 0.0004, p_{int} = 0.047) (Table 3). None of these interactions remained statistically significant after FDR correction. The corresponding dose–response analysis showed that normal sperm morphology declined with increasing ACY concentration at both low (25th percentile) and high (75th percentile) Cu levels, with a steeper decline observed at the higher Cu level (Figure S4b). In contrast, normal sperm morphology increased with increasing PYR concentration at both Cu levels, with a more pronounced increase observed at the lower Cu level (Figure S4c). Similarly, normal sperm morphology increased with increasing FLA concentration when Cu was fixed at its lower level, whereas it decreased when Cu was fixed at its higher level (Figure S4d). Normal sperm morphology declined with increasing PHE concentration at both Cu levels, with a steeper decline

observed at the higher Cu level (Figure S4e). The dose–response analysis further showed that normal sperm morphology increased with increasing B[k]F concentration when Se was fixed at its higher level (75th percentile), whereas it declined when Se was fixed at its lower level (25th percentile) (Figure S4f).

In terms of vitality, a nominally significant negative interaction was identified between B[ghi]P and Cu (β_{int} = −0.00002, p_{int} = 0.018) (Table 3). However, this interaction did not remain significant after FDR correction. The corresponding dose–response analysis showed that sperm vitality declined with increasing B[ghi]P concentration when Cu was fixed at its higher level (75th percentile), whereas a slight increasing trend was observed when Cu was fixed at its lower level (25th percentile) (Figure S5b).

In terms of DNA fragmentation, nominally significant negative interactions were identified between Se and B[a]A (β_{int} = −0.00006, p_{int} = 0.001) and between Se and B[b]F (β_{int} = −0.00006, p_{int} = 0.033) (Table 3). The B[a]A-Se interaction remained statistically significant after FDR correction (adjusted p-value = 0.048), whereas the B[b]F-Se interaction did not. The dose–response analysis showed that sperm DNA fragmentation increased with increasing B[a]A (Figure 1b) and B[b]F concentrations at both low (25th percentile) and high (75th percentile) Se levels, with a more pronounced increase observed at the lower Se level (Figure 1c).

3.4. Model Diagnostics and Sensitivity Analyses

Spearman correlation analyses indicated moderate-to-strong correlations among several PAHs, whereas correlations among the metals were generally more moderate (Figure 2). GVIF analyses were additionally used to assess potential multicollinearity among the exposure variables within the fitted interaction models (Table S7). Taken together, the correlation and GVIF results suggested that collinearity among some exposure variables may have increased the variability of the estimated model coefficients. In sensitivity analyses excluding adjustment for the remaining PAHs and metals, most interaction estimates retained the same direction as those from the primary models, although their magnitudes and statistical significance varied across model specifications (Table S11), indicating that some interaction estimates were sensitive to co-exposure adjustment. Cook's distance diagnostics showed that a relatively small number of data points may potentially influence individual observations in the fitted interaction models (Table S12). These diagnostic and sensitivity analyses were considered when interpreting the interaction findings.

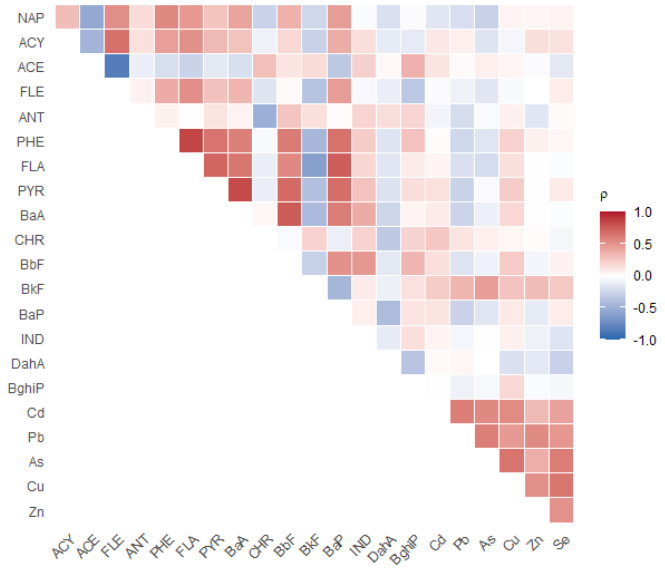


Figure 2. Spearman correlation heatmap of PAH and metal concentrations.

4. Discussion

Currently, few studies have examined the interactions between PAHs and both xenobiotic and essential metals in relation to sperm quality, largely due to methodological, analytical, logistical, sampling, and cost-related challenges associated with studying these complex co-exposures. Despite its exploratory nature, this study is among the few to overcome these challenges and to provide empirical evidence assessing the interactions between PAHs and metals in relation to sperm quality, highlighting the potential public health implications of these complex environmental co-exposures.

Several associations between the PAH–metal interactions and sperm quality were observed. They reached nominal significance ($p_{raw} < 0.05$) but did not survive FDR correction ($p_{FDR} \geq 0.05$). While these signals of the associations align with the theoretical framework and biological plausibility, they cannot be distinguished from background noise or Type I error within the context of our multi-hypothesis testing framework [18]. Consequently, these non-FDR-surviving associations should be interpreted strictly as exploratory or hypothesis-generating candidate targets rather than definitive discoveries. This cautious interpretation is further supported by sensitivity analyses, in which the direction of most interaction estimates was maintained, but the magnitude and statistical significance of some estimates varied across model specifications. Future studies utilizing larger, independently powered cohorts and targeted single-hypothesis testing designs are required to confirm whether these observed effect sizes represent true underlying populations.

Our findings provide important guidance for future studies. First, they help identify a shortlist of candidate PAHs and metals for follow-up investigation. In future studies, focusing specifically on these high-priority candidates can allow researchers to conduct targeted mechanistic and confirmatory experiments rather than screening a large number of compounds simultaneously. For such hypothesis-driven confirmatory studies, the conventional statistical significance threshold (e.g., $p < 0.05$) may be sufficient when testing prespecified targets, without necessarily requiring FDR correction. Second, as noted above, few studies have examined these interactions, in part because large-scale validation studies are expensive and time-consuming. Our findings therefore provide a valuable resource for prioritizing targets and leveraging empirical evidence to narrow the focus to PAHs and metals with the strongest evidence of potential biological interactions. Third, even when individual features do not survive FDR correction, clusters of nominally significant associations may reveal underlying biological or structural coherence. For example, interactions between PAHs and essential metals exhibited consistent negative dose–response relationships. These patterns were consistent with the B[a]A–Se interaction that remained significant after FDR correction. In particular, PAH–Se interactions involving similar functional pathways repeatedly demonstrated nominal significance, suggesting that the collective enrichment of these interactions may have biological relevance. Overall, these findings provide a strong foundation for future studies investigating secondary biological pathways and the potential mechanisms underlying PAH–metal interactions in male reproductive toxicity.

Our primary analysis indicated that Se modified the association between B[a]A and DNA fragmentation. Sperm DNA fragmentation decreased with increasing B[a]A exposure when Se levels were higher. B[a]A is classified as a high-priority toxicant due to its lipophilic nature, bioaccumulative potential, and ability to disrupt reproductive physiology. Upon entering cells, BaA binds to the aryl hydrocarbon receptor (AhR), inducing the expression of phase I metabolic enzymes, including CYP1A1 and CYP1B1 [21,22]. The metabolic conversion of BaA generates reactive epoxides, dihydrodiols, and quinones, which can induce single- and double-strand DNA breaks and the formation of oxidative DNA adducts [23]. An additional and potentially important mechanism of B[a]A toxicity

is its ability to cause a transient, early depletion of intracellular reduced glutathione (GSH) [22,23]. B[a]A targets specific cellular amino acid transporters, impairing glutamate uptake and thereby disrupting GSH synthesis. The resulting depletion of GSH can promote substantial lipid hydroperoxide accumulation and impair the detoxification of reactive diol-epoxide metabolites, potentially increasing oxidative stress and DNA damage [24].

Se may counteract B[a]A-induced male reproductive toxicity through its role in the glutathione (GSH)-dependent antioxidant and detoxification system [25,26]. As an essential trace element, Se is required for the synthesis and activity of selenoproteins [27,28], particularly glutathione peroxidases (GPx), which use reduced glutathione (GSH) to neutralize ROS and limit oxidative damage [29]. Through supporting GPx activity and GSH-dependent antioxidant defenses, Se may also facilitate the detoxification and clearance of reactive B[a]A metabolites generated during Phase I metabolism, thereby reducing oxidative stress and subsequent reproductive toxicity. Adequate Se status optimizes GPx catalytic kinetics (GPx-Se^-/GPx-SeOH), accelerating the recycling loop and maintaining the availability of GSH for cellular defense rather than allowing GSH pools to become depleted. This may help prevent B[a]A-induced oxidative stress (low GSH:GSSG ratio) in testicular cells and maintain a more favorable redox state, reflected by a higher GSH ratio [19,25].

A consistent pattern was observed in which PAHs and heavy metals had interactive, negative associations with sperm morphology, vitality, and motility in the primary analysis. Decreased sperm vitality, normal morphology, and motility were observed with increasing levels of PAHs (e.g., B[ghi]P and ACY), particularly when concentrations of heavy metals such as Cd and As were higher. However, some of these interaction estimates attenuated the magnitude of the significance. Due to the exploratory nature of this study, causal effects cannot be definitively established. However, previous epidemiologic studies have provided evidence that co-exposure to B[ghi]P and Cd may substantially impair sperm quality through synergistic oxidative stress and alterations in cellular structure [11,30].

When interpreting these findings, several study limitations should be considered. First, the cross-sectional design precludes causal inference. Nevertheless, this design was appropriate for examining interactions between metals and PAHs and characterizing dose–response patterns, which were consistent with changes in sperm quality status. Second, the relatively small sample size limited the application of advanced statistical approaches, such as kernel machine regression, to evaluate complex, non-additive mixture effects. Also, the sample size may not minimize false significant positives due to multiple testing of the large number of PAH–metal combinations evaluated. The Benjamini–Hochberg FDR procedure was employed in this study to address this concern. Third, the modest sample size and correlations among concurrent exposures may have increased the variability and sensitivity of individual interaction estimates. Although sensitivity analyses using reduced models with alternative co-exposure adjustment were conducted, some interaction estimates varied across model specifications, and influence diagnostics indicated sensitivity of some fitted models to individual observations. Given the exploratory nature of the interaction analyses and the complexity of the observed interactions, these findings were interpreted cautiously and conservatively.

5. Conclusions

Se was found to be associated with the association between B[a]A exposure and sperm DNA fragmentation. Several PAHs and metals were identified as potential priority candidates for further investigation in larger-scale studies.

Supplementary Materials: The following supporting information can be downloaded at https://www.mdpi.com/article/10.3390/jox16070207/s1, Figure S1. Dose–response trends between PYR, B[a]A, and B[b]F and sperm concentration by Cd exposure levels. Figure S2. Dose–response trends between NAP, IND, B[a]A, and D[ah]A and sperm concentration by Pb exposure levels. Figure S3. Dose–response trends between B[ghi]P and sperm motility at low and high levels of interacting xenobiotic and essential metals. Figure S4. Dose–response trends between PAH exposures and normal sperm morphology by both xenobiotic and essential metal exposure levels. Figure S5: Dose–response trends between B[ghi]P exposure and sperm vitality by both xenobiotic and essential metal exposure levels. Figure S6: Dose–response trends between NAP and ACY exposures and sperm concentration at different levels of essential metal exposure. Table S1. Interaction effects between PAH metabolites and heavy metals in relation to sperm concentration. Table S2. Interaction effects between PAH metabolites and heavy metals in relation to motility. Table S3. Interaction effects between PAH metabolites and essential metals in relation to motility. Table S4. Interaction effects between PAH metabolites and essential metals in relation to sperm concentrations. Table S5. Interaction effects between PAH metabolites and heavy metals in relation to vitality. Table S6. Interaction effects between PAH metabolites and essential metals in relation to vitality. Table S7. Interaction effects between PAH metabolites and heavy metals in relation to normal morphology. Table S8. Interaction effects between PAH metabolites and essential metals in relation to normal morphology. Table S9. Interaction effects between PAH metabolites and heavy metals in relation to sperm DNA fragmentation. Table S10. Interaction effects between PAH metabolites and essential metals in relation to sperm DNA fragmentation. Table S11. Sensitivity analysis comparing PAH–metal interaction estimates from the primary fully adjusted models and reduced models. Table S12. Multicollinearity and influence diagnostics for the PAH–metal interaction models.

Author Contributions: Conceptualization, H.A.J.; methodology, H.A.J., S.S. and C.-H.P.; software, S.S.; Validation, S.S.; Investigation, H.A.J.; Resources, H.A.J.; Data curation, H.A.J. and C.-H.P.; Writing—original draft, H.A.J.; Writing—review & editing, S.S.; Visualization, S.S.; Project administration, H.A.J.; Funding acquisition, H.A.J. All authors have read and agreed to the published version of the manuscript.

Funding: This work was partially supported by the US National Institute of Environmental Health Sciences (1R15ES018952-01).

Institutional Review Board Statement: The study was approved by the Institutional Review Board of Old Dominion University for studies involving humans (protocol code 395071, date of approval: 17 May 2014).

Informed Consent Statement: Informed consent was obtained from all subjects involved in the study.

Data Availability Statement: The original contributions presented in this study are included in the article/Supplementary Material. Further inquiries can be directed to the corresponding author.

Conflicts of Interest: The authors declare no conflicts of interest.

Abbreviations

The following abbreviations are used in this manuscript:

PAHs	Polycyclic aromatic hydrocarbons
NAP	Naphthalene
ACY	Acenaphthylene
ACE	Acenaphthene
FLE	Fluorene
PHE	Phenanthrene
ANT	Anthracene
PRY	Pyrene
FLA	Fluoranthene
B[a]A	Benzo[a]anthracene

CHR	Chrysene
B[b]F	Benzo[b]fluoranthene
B[k]F	Benzo[k]fluoranthene
B[a]P	Benzo(a)pyrene
IND	Indeno[1,2,3-cd]pyrene
D[ah]A	Dibenzo[a,h]anthracene
B[ghi]P	Benzo[ghi]perylene
TUNEL	Terminal deoxynucleotidyl transferase-mediated dUTP nick-end labeling

References

1. Levine, H.; Jørgensen, N.; Martino-Andrade, A.; Mendiola, J.; Weksler-Derri, D.; Mindlis, I.; Pinotti, R.; Swan, S.H. Temporal trends in sperm count: A systematic review and meta-regression analysis. *Hum. Reprod. Update* **2017**, *23*, 646–659. [CrossRef]
2. Swan, S.H.; Elkin, E.P.; Fenster, L. The question of declining sperm density revisited: An analysis of 101 studies published 1934–1996. *Environ. Health Perspect.* **2000**, *108*, 961–966. [CrossRef]
3. Galarneau, E. Source apportionment of atmospheric polycyclic aromatic hydrocarbons (PAHs) using diagnostic ratios: A review. *Atmos. Environ.* **2008**, *42*, 8139–8149.
4. Latifi, A.M.; Abdi, M.; Miri, M.; Ashtari, S.; Ghalandarpoor-Attar, S.N.; Mohamadzadeh, M.; Fouladi, A.A.I.; Uddin, S. Association between exposure to polycyclic aromatic hydrocarbons and reproductive health outcomes: A systematic review and meta-analysis. *J. Health Popul. Nutr.* **2025**, *30*, 382. [CrossRef]
5. Montano, L.; Baldini, G.M.; Piscopo, M.; Liguor, I.G.; Lombardi, R.; Ricciardi, M. Polycyclic aromatic hydrocarbons (PAHs) in the environment: Occupational exposure, health risks and fertility implications. *Toxics* **2025**, *13*, 151. [CrossRef]
6. Azil, S.; Errafii, K.; Benkhalifa, M.; Louanjli, N.; Ghazi, B.; Hamdi, S. A narrative review of heavy metals and sperm quality: The interplay with antioxidant imbalance and reactive oxygen species. *Curr. Issues Mol. Biol.* **2025**, *47*, 650. [CrossRef]
7. Mu, M.; Xiong, S.; Guan, X.; Yu, L.; Guo, H.; Lai, X. Associations of co-exposure to metals and polycyclic aromatic hydrocarbons with aging biomarkers: Insights from epidemiology and network toxicology. *Front. Public Health* **2026**, *28*, 1844457. [CrossRef]
8. Ren, Y.; Wang, Y.; Wang, Y.; Ning, X.; Li, G.; Sang, N. Exposure to oxygenated polycyclic aromatic hydrocarbons and endocrine dysfunction: Multi-level study based on hormone receptor responses. *J. Hazard. Mater.* **2025**, *485*, 136855. [CrossRef]
9. Goutam Mukherjee, A.; Ramesh Wanjari, U.; Eladl, M.A.; El-Sherbiny, M.; Elsherbini, D.M.A.; Sukumar, A.; Kannampuzha, S.; Ravichandran, M.; Renu, K.; Vellingiri, B.; et al. Mixed Contaminants: Occurrence, Interactions, Toxicity, Detection, and Remediation. *Molecules* **2022**, *27*, 2577. [CrossRef]
10. Gauthier, P.T.; Norwood, W.P.; Prepas, E.E.; Pyle, G.G. Metal–PAH mixtures in the aquatic environment: A review of co-toxic mechanisms leading to more-than-additive outcomes. *Aquat. Toxicol.* **2014**, *154*, 253–269. [CrossRef]
11. Nayak, J.; Jena, S.R.; Kumar, S.; Kar, D.; Dixit, A.; Samanta, L. Human sperm proteome reveals the effect of environmental borne seminal polyaromatic hydrocarbons exposome in etiology of idiopathic male factor infertility. *Front. Cell Dev. Biol.* **2023**, *11*, 1117155. [CrossRef]
12. Wang, T.; Feng, W.; Kuang, D.; Deng, Q.; Zhang, W.; Wang, S. The effects of heavy metals and their interactions with polycyclic aromatic hydrocarbons on the oxidative stress among coke-oven workers. *Environ. Res.* **2015**, *140*, 405–413. [CrossRef]
13. Stella, A.; Piccardo, M.T.; Pala, M.; Balducci, D.; Cipolla, M.; Ceppi, M. Temporal and spatial variations of polycyclic aromatic hydrocarbon concentrations around a coke oven plant. *J. Air Waste Manag. Assoc.* **2012**, *62*, 1003–1011. [CrossRef]
14. Jeng, H.A.; Pan, C.H.; Chao, M.R.; Chiu, C.C.; Zhou, G.; Chou, C.K.; Lin, W.Y. Sperm quality and DNA integrity of coke oven workers exposed to polycyclic aromatic hydrocarbons. *Int. J. Occup. Med. Environ. Health* **2016**, *29*, 915–926. [CrossRef]
15. Shang, D.; Kim, M.; Haberl, M. Rapid and sensitive method for the determination of polycyclic aromatic hydrocarbons in soils using pseudo multiple reaction monitoring gas chromatography/tandem mass spectrometry. *J. Chromatogr. A* **2014**, *1334*, 118–125. [CrossRef]
16. World Health Organization. *WHO Laboratory Manual for the Examination and Processing of Human Semen*, 6th ed.; World Health Organization: Geneva, Switzerland, 2021. Available online: https://www.who.int/publications/i/item/9789240030787 (accessed on 15 February 2026).
17. Björndahl, L.; Barratt, C.L.; Mortimer, D.; Agarwal, A.; Aitken, R.; Alvarez, J.G.; Aneck-Hahn, N.; Arver, S.; Baldi, E.; Bassas, L.; et al. Standards in semen examination: Publishing reproducible and reliable data based on high-quality methodology. *Hum. Reprod.* **2022**, *7*, 2497–2502. [CrossRef]
18. Kyrylkova, K.; Kyryachenko, S.; Leid, M.; Kioussi, C. Detection of apoptosis by TUNEL assay. *Methods Mol. Biol.* **2012**, *887*, 41–47. [CrossRef]
19. Bermingham, E.N.; Hesketh, J.E.; Sinclair, B.R.; Koolaard, J.P.; Roy, N.C. Selenium-enriched foods are more effective at increasing glutathione peroxidase (GPx) activity compared with selenomethionine: A meta-analysis. *Nutrients* **2014**, *6*, 4002–4031. [CrossRef]

20. Storey, J.D. A direct approach to false discovery rates. *J. R. Stat. Soc. Ser. B (Stat. Methodol.)* **2002**, *64*, 479–498. [CrossRef]
21. Stoddard, E.G.; Killinger, B.J.; Nag, S.A.; Martin, J.; Corley, R.; Smith, J.N.; Wright, A.T. Benzo[a]pyrene induction of glutathione S-transferases: An activity-based protein profiling investigation. *Chem. Res. Toxicol.* **2019**, *32*, 1259–1267. [CrossRef]
22. Valencia-Cervantes, J.; Sierra-Vargas, M.P. Benz[a]anthracene exposure from e-cigarettes and its association with lung carcinogenesis. *Neumol. Cirugía. Tórax.* **2023**, *82*, 225–231.
23. Seike, K.; Murata, M.; Oikawa, S.; Hiraku, Y.; Hirakawa, K.; Kawanishi, S. Oxidative DNA damage induced by benz[a]anthracene metabolites via redox cycles of quinone and unique non-quinone. *Chem. Res. Toxicol.* **2003**, *16*, 1470–1476. [CrossRef]
24. Watanabe, N.; Dickinson, D.A.; Liu, R.M.; Forman, H.J. Quinones and glutathione metabolism. *Methods Enzymol.* **2004**, *378*, 319–340. [CrossRef]
25. Hsiao, Y.-F.; Huang, S.-C.; Cheng, S.-B.; Hsu, C.-C.; Huang, Y.-C. Glutathione and selenium supplementation attenuates liver injury in diethylnitrosamine-induced hepatocarcinogenic mice by enhancing glutathione-related antioxidant capacities. *Int. J. Mol. Sci.* **2024**, *25*, 11339. [CrossRef]
26. Bai, Y.; Feng, W.; Wang, S.; Zhang, X.; Zhnag, W.; He, M. Essential metals zinc, selenium, and strontium protet against chromosome damage caused by polycyclic aromatic hydroarbons exposure. *Environ. Sci. Technol.* **2016**, *50*, 951–960. [CrossRef]
27. Bulteau, A.-L.; Chavatte, L. Update on selenoprotein biosynthesis. *Antioxid. Redox Signal.* **2015**, *23*, 797–812. [CrossRef]
28. Howard, M.T.; Carlson, B.A.; Anderson, C.B.; Hatfield, D.L. Translational recoding: Coordination of UGA codon decoding with tRNA modification and selenoprotein synthesis. *Biochim. Biophys. Acta* **2013**, *1830*, 3608–3616.
29. Ringuet, M.T.; Hunne, B.; Lenz, M.; Bravo, D.M.; Furness, J.B. Analysis of bioavailability and induction of glutathione peroxidase by dietary nanoelemental, organic and inorganic selenium. *Nutrients* **2021**, *13*, 1073. [CrossRef]
30. Shi, Y.; Gaurab, P.; Wang, W.; Yan, J.; Sun, Z.; Zhang, Y.; Liu, J.; Liu, X.; Zhang, D. Interaction effect of polycyclic aromatic hydrocarbon metabolites and cadmium on semen quality in nonsmokers. *Environ. Sci. Pollut. Res.* **2020**, *27*, 33990–33997. [CrossRef]

Disclaimer/Publisher's Note: The statements, opinions and data contained in all publications are solely those of the individual author(s) and contributor(s) and not of MDPI and/or the editor(s). MDPI and/or the editor(s) disclaim responsibility for any injury to people or property resulting from any ideas, methods, instructions or products referred to in the content.